

Segmentation of Micro-Doppler Signatures of Human Sequential Activities using Rényi Entropy

Kruse, Nicolas; Guendel, Ronny; Fioranelli, Francesco; Yarovoy, Alexander

DOI

[10.1049/icp.2022.2357](https://doi.org/10.1049/icp.2022.2357)

Publication date

2022

Document Version

Final published version

Published in

IET Conference Proceedings

Citation (APA)

Kruse, N., Guendel, R., Fioranelli, F., & Yarovoy, A. (2022). Segmentation of Micro-Doppler Signatures of Human Sequential Activities using Rényi Entropy. In *IET Conference Proceedings* (17 ed., Vol. 2022, pp. 435-440). Institution of Engineering and Technology. <https://doi.org/10.1049/icp.2022.2357>

Important note

To cite this publication, please use the final published version (if applicable). Please check the document version above.

Copyright

Other than for strictly personal use, it is not permitted to download, forward or distribute the text or part of it, without the consent of the author(s) and/or copyright holder(s), unless the work is under an open content license such as Creative Commons.

Takedown policy

Please contact us and provide details if you believe this document breaches copyrights. We will remove access to the work immediately and investigate your claim.

Green Open Access added to TU Delft Institutional Repository

'You share, we take care!' - Taverne project

<https://www.openaccess.nl/en/you-share-we-take-care>

Otherwise as indicated in the copyright section: the publisher is the copyright holder of this work and the author uses the Dutch legislation to make this work public.

Segmentation of Micro-Doppler Signatures of Human Sequential Activities using Rényi Entropy

Nicolas Kruse*, Ronny Guendel, Francesco Fioranelli, Alexander Yarovoy

Microwave Sensing, Signals and Systems (MS3), Delft University of Technology, Delft, The Netherlands

*E-mail: n.c.kruse@tudelft.nl

Keywords: SEGMENTATION, HUMAN ACTIVITY RECOGNITION, MICRO-DOPPLER, RÉNYI ENTROPY

Abstract

Classifying continuous sequences of human activities is a current research challenge due to the unconstrained duration of the constituent activities. Segmentation of these sequences into single-activity segments is under investigation as a potential solution to this challenge and has been studied in this work. A segmentation method has been proposed based on the extracted Rényi entropy of micro-Doppler spectrogram representations of human motion. The proposed method has been compared to a state of the art method for three different experimental data sets, for various sequence types, and in varying signal-to-noise regimes. It has been shown that the performance of the proposed method is up to $55 \pm 22\%$ higher than the reference method when applied to different data sets with unchanged parameters. Additionally, improved performance under degraded signal-to-noise ratio (SNR) conditions has been demonstrated for the proposed method. Finally, two methods for sensor fusion have been formulated for enhanced segmentation performance when multiple radar nodes are available, and have been demonstrated to increase performance by up to $10 \pm 2\%$. The improved segmentation performance is expected to lead to improvements in continuous activity classification.

1 Introduction

Monitoring human activities with radar is an active field of research due to the advantageous characteristics of radar sensing over alternative sensors. The non-contact, all-visibility, privacy preserving nature of radar observations is a valuable prospect for e.g. healthcare, where potential applications include vital sign monitoring [1, 2], gait analysis [3], fall detection [4, 5], and activity classification [5–10].

In the case of activity classification, the major challenge is the step from classifying single, isolated activities, to classifying continuous sequences containing various activities of unconstrained duration performed successively. One method of attempting to tackle this challenge is the segmentation of a continuous sequence of activities into its constituent single activity parts. This process of segmentation is often performed based on brief pauses inserted between subsequent activities [11, 12], or on other notable changes in the observed motion [13].

In this work, a segmentation method is proposed based on a statistical descriptor of the activity sequence, namely the Rényi entropy. It is expected that entropy will better reflect changes in motion types, rather than solely their presence or absence. The proposed method is compared with a state of the art method [13] from literature and evaluated over three different experimental data sets, and under varying signal-to-noise conditions. A performance metric is proposed to quantify segmentation performance. The proposed method is shown to have higher average performance over the three data sets when parameters are kept unchanged, indicating that re-optimisation of parameters per data set is less necessary than

for the reference method. Better performance is also demonstrated in degraded signal-to-noise conditions. Additionally, sensor fusion methods are proposed and verified with an experimental data set, collected with a network of five radars. Here, performance improvement is also shown.

The main contributions in this work are as follows:

- Introduction of a novel method for human activity sequence segmentation based on Rényi entropy.
- Application of the proposed segmentation method and an alternative method from the literature to 3 different experimental data sets, with subsequent performance evaluation.
- Analysis of sensor fusion methods for segmentation performance improvement when data from multiple radars are available.

In Section 2 the utilised data sets and relevant processing steps are described, followed by a formulation of the segmentation methods in Section 3. Aspects related to the performance evaluation of the segmentation methods are outlined in Section 4. Section 5 contains the results of performed experiments, with conclusions in section 6.

2 Data Acquisition and Pre-Processing

In what follows, the data used in this work are described, as well as relevant pre-processing steps. Data sets containing sequences of human activities from three sources are utilised: a set collected by researchers from the University of Alabama (ALA) [13], a set collected by researchers from the University of Glasgow (GLG) [14], and a set collected by researchers from

Table 1 Description of data sets (top), and specific sequence types in the TUD data set (bottom).

ALA	University of Alabama data set [13]	Data set containing sequential motions of 3 daily activities (walking, sitting, standing up) and 15 ASL signs. 12 Subjects.
GLG	University of Glasgow data set [14]	Data set including sequences of 6 human activities, namely walking, sitting on a chair, standing up, bending to pick up an object, drinking a glass of water, and simulating a frontal fall. 16 Subjects.
TUD	Delft University of Technology data set [15]	Data set of 9 human activities including, among others, walking, sitting, and falling. Seven sequence types are collected, five of which are described in the lower part of this table. 15 Subjects
	- Walk and Stop	Walking and stopping at random intervals
	- Walk and Fall	Walking and falling randomly, repeatedly
	- Sit	Sitting down and standing up, repeatedly
'029'	Fixed location mix	Mix of all activity classes, performed in fixed locations (± 1 m)
'030'	Random location mix	Mix of all activity classes, performed in random locations in the area of observation

the Delft University of Technology (TUD) [15]. Descriptions of these data sets are found in Table 1.

2.1 TUD Data Set

The TUD data set is acquired by means of a set of five PulsON P410 Ultra Wideband radars with a centre frequency and bandwidth of 4.3 GHz and 2.2 GHz respectively. The monostatic, omnidirectional radars are arranged in a semicircle with a diameter of 6.38 m, where a concentric circle of diameter 4.38 m is designated as the area of observation. A variety of activities are performed in this area, in sequences of 120 seconds in duration. The sequences are manually labelled, resulting in a ground truth signal of activity labels accompanying every sequence. The sequence names and descriptions can be found in Table 1. This data set has been made publicly available [15].

Each of the five pulse radar nodes outputs a real-valued vector corresponding to the back-scattered signal. A Hilbert transform is applied, resulting in a complex-valued IQ vector which is reshaped into a matrix with short-time and long-time dimensions. A Fast Fourier Transform (FFT) is subsequently performed across the short-time dimension of the complex-valued matrix. From this FFT, the frequency bin corresponding to the centre frequency of 4.3 GHz is isolated and a Short-Time Fourier Transform (STFT) is performed on this complex vector. For the STFT a Hanning window of 128 samples with an overlap of 120 samples is used, with a sample time of 8.2 ms. The magnitude of the complex-valued STFT will hereafter be referred to as the spectrogram, and will be denoted as \mathbf{X} or X_{mn} , with m indicating Doppler frequency index and n indicating time index. Examples of spectrograms can be viewed in Guendel et al., 2022 [8].

3 Sequence Segmentation

In this section, two methods are described for the segmentation of a sequence of human activities into individual activities.

Both methods function by locating transition points in spectrograms, which can be used to segment the input sequence.

3.1 Proposed Method

The sequence segmentation method proposed in this work relies at its core on the detection of rapid fluctuations in signal entropy. The motivation for entropy as a descriptor is that it is expected to grant a better insight in the nature of an input signal compared to alternative quantities such as the Power Burst Curve (PBC) [9, 13]. Specifically, the Rényi Entropy H_α [16] is first extracted as in [17] from an input spectrogram \mathbf{X} after normalising every time bin \mathbf{X}_n separately:

$$H_\alpha(\mathbf{X}_n) = \frac{1}{1-\alpha} \log \left(\sum_m \left(\frac{X_{mn}}{\sum_m X_{mn}} \right)^\alpha \right) \quad (1)$$

for $\alpha \geq 0$ and $\alpha \neq 1$. Here X_{mn} indicates the m th frequency bin of the n th time bin. In this representation, every time bin of the input spectrogram is treated as a probability distribution whose entropy can be computed, with frequency as the discrete random variable and the normalised spectral magnitude as the probability. The parameter α governs the extent to which large probabilities influence the entropy, with entropy values dominated by high-probability events for larger values of α . Computing (1) for all time bins results in a discrete 1-D time series $H_\alpha[t]$ for a given spectrogram.

To detect rapid changes in entropy, a difference threshold over a fixed time interval is utilised:

$$|H_\alpha[t] - H_\alpha[t + T_{lag}]| \geq \beta \sigma_H \quad (2)$$

with T_{lag} the time interval, σ_H the standard deviation of the entropy over the duration of the sequence, and β a multiplicative factor. A multiple of the entropy standard deviation is chosen to couple the segmentation parameters to the input data as much as possible, and to minimise the necessity of fine-tuning parameters per data set. Whenever the threshold from inequality (2) is exceeded, a transition point is declared and stored at that time instant.

3.2 STA/LTA Segmentation

As a primary comparison to the proposed method, 'short term average over long time average' (STA/LTA) is utilised as a change detection algorithm. Following [13], the upper and lower envelopes \mathbf{u} and \mathbf{l} of a spectrogram \mathbf{X} are computed by setting the cumulative sum of the magnitudes in a time bin to 95 % and 5 % of the total respectively and solving for the corresponding frequency bins. The absolute distance between the upper and lower envelope $\mathbf{b} = |\mathbf{u} - \mathbf{l}|$ will hereafter be referred to as the bandwidth of the spectrogram and is denoted as a discrete function of time $b[t]$. The short term average and long term average of the bandwidth at a time t are given by

$$STA[t] = \frac{1}{T_S} \sum_{t'=t}^{t+T_S} b[t']$$

$$LTA[t] = \frac{1}{T_L} \sum_{t'=t-T_L}^t b[t']$$

respectively, with T_S and T_L indicating the length of the short and long windows respectively. Starting and ending points of activities in the sequence are indicated by two sets of conditions respectively:

$$STA[t] > \sigma_1 \ \& \ \frac{STA[t]}{LTA[t]} > \sigma_2$$

$$STA[t] < \sigma_3 \ \& \ \frac{STA[t]}{LTA[t]} < \sigma_2.$$

A STA/LTA ratio exceeding σ_2 indicates that a change in the signal is occurring. Parameter σ_1 is a threshold to prevent noise from triggering the start of a segment, and σ_3 is in place to delay the end of the segment until a given motion has ceased sufficiently.

4 Case Studies

In the current section, aspects related to the evaluation and comparison of the segmentation methods are presented.

4.1 Performance Metric

In order to compare segmentation effectiveness, a performance metric is proposed here that evaluates both the quantity of found transition points, as well as their proximity to ground truth transitions. This dimensionless metric will be used throughout this work. A trapezoidal scoring function is defined around each ground truth transition such that a found transition at time t_i is assigned a score of:

$$f[t_i] = \begin{cases} 1, & |t_i - t_j^{GT}| < T_{tol} \\ 1 - \frac{|2(t_i - t_j^{GT}) - T_{tol}|}{T_{tol}}, & T_{tol} \leq |t_i - t_j^{GT}| \leq \frac{3}{2}T_{tol} \\ 0, & \text{otherwise} \end{cases} \quad (3)$$

where t_j^{GT} indicates the j th ground truth transition point and T_{tol} is a tolerance region around this point. Figure 1 graphically

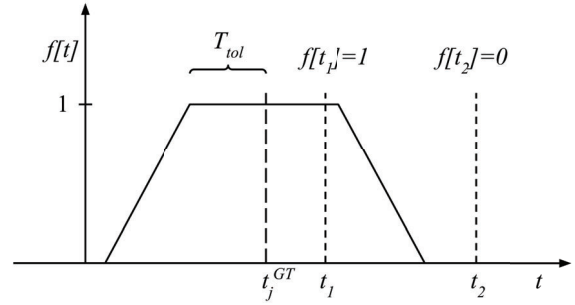


Fig. 1 Graphical representation of the performance metric function and related quantities.

represents the function and its related quantities. The tolerance region allows for small deviations of found transitions from ground truth transitions not to be penalised. This tolerance region helps for example to negate the effects of human error in ground truth labelling, as well as that of the subjective notion of the exact location of a transition point between two activities. The tolerance region is empirically set to 1s based on visual inspection of ground truth labels and corresponding spectrograms. Only the found transition in closest proximity to a ground truth transition receives a score $f[t_i]$, all other transitions automatically receive a score of $f[t_i] = 0$ unless they can be associated with a different ground truth transition. A single found transition can only be matched to a maximum of one ground truth transition. The scores for all found transitions are summed and divided by the total amount of ground truth transitions, j_{max} , or the total amount of found transitions, i_{max} , whichever is greater:

$$S = \frac{\sum_i f[t_i]}{\max\{i_{max}, j_{max}\}}. \quad (4)$$

These operations result in a score $S \in [0, 1] \subset \mathbb{R}$ for a set of found transitions that rewards both timeliness and quantity of found transitions.

4.2 Signal Fusion

As described in Section 2.1, the activities in the TUD data set are observed by a network of five radar nodes simultaneously. To investigate the effectiveness of sensor fusion for segmentation performance increase, two methods of signal fusion are proposed here. Consider a set of spectrograms G originating from a corresponding combination of radar nodes. For the first method, *fusion through summation*, spectrograms are summed element-wise over this set:

$$F_{mn} = \sum_{X \in G} X_{mn} \quad (5)$$

where F is the final, fused spectrogram. The second fusion method entails the *concatenation of the spectrograms* of interest in the frequency dimension, such that

$$F_n = X_n \hat{\wedge} Y_n \hat{\wedge} \dots \hat{\wedge} Z_n, \quad X, Y, Z \in G, \quad (6)$$

where the subscript n indicates the n th time bin of a spectrogram and the operator $\hat{\cdot}$ indicates concatenation. For both methods, the fused spectrogram \hat{F} is subsequently utilised as the input for further segmentation processing as in Section 3.1.

4.3 Method Optimisation

In order to be able to compare the two methods described in Section 3, an optimisation of their parameters is performed under various conditions. Optimisation is achieved by means of a Genetic Algorithm (GA) intended to maximise the performance within each method's parameter space. Specifically, the GA from the Global Optimization Toolbox for MATLAB is employed with default parameters except for the stopping condition, which is set to a total run time of 2 hours. The average improvement per iteration after this time is noted to be less than a percent of typical standard deviations of performance between sequences. As discussed in section 3.2, the parameters for STA/LTA segmentation are the noise thresholds σ_1 and σ_3 , the ratio threshold σ_2 , and the two window sizes T_1 and T_2 . For the proposed method, the parameters are the entropy parameter α , and the lag window size T_{lag} .

5 Results

In this section the results of several experiments are presented.

In Tables 2 and 3, an investigation in the optimality of method parameters and their portability between different data sets and sequences is summarised. The parameters of each method are optimised for a particular data set or sequence type, and subsequently applied to the remaining data sets or sequence types. It should be noted that parameters are scaled where applicable, e.g. window sizes for differing sample rates. The off-diagonal elements in both tables reflect the portability of optimised parameters across different data sets. It is noted that the proposed method generally results in higher performance than its STA/LTA counterpart. Additionally, it can be seen that the lowest performance elements in both tables are associated with the Glasgow data set, indicating general difficulties in automatically segmenting these sequences.

Table 2 Segmentation performance for the proposed method, with parameters optimised for one out of four sets of sequences and subsequently applied to all four sets to gauge portability of parameters. Subscripts 'W' and 'M' refer to sequence types *Walk and Stop*, and '*mix 030*' respectively. Refer to Table 1 for sequence descriptions.

[%]	Optimised for:			
	TUD _W	TUD _M	ALA	GLG
TUD _W	91±7	83±11	61±13	72±13
Applied TUD _M	59±12	74±10	57±9	46±8
on: ALA	40±10	75±12	80±10	39±11
GLG	53±16	48±10	36±7	62±14

Figure 2 summarises the results of the sensor fusion experimental work. The fusion methods from Section 4.2 are applied

Table 3 Segmentation performance for the STA/LTA-based method, with parameters optimised for one out of four sets of sequences and subsequently applied to all four sets to gauge portability of parameters. Subscripts 'W' and 'M' refer to sequence types *Walk and Stop*, and '*mix 030*' respectively. Refer to Table 1 for sequence descriptions.

[%]	Optimised for:			
	TUD _W	TUD _M	ALA	GLG
TUD _W	87±10	76±10	41±11	17±15
Applied TUD _M	56±14	76±10	44±6	14±11
on: ALA	51±17	76±12	84±8	24±11
GLG	4±8	6±13	47±9	64±15

to the *Walk and Stop* and '*mix 030*' sequences, before being processed with the proposed segmentation method. The results indicate that the spectrogram summation method exhibits the most notable effect on performance, with an improvement of $7 \pm 3\%$ in the case of walking and stopping when increasing from one node to two nodes. Further increases in amount of fused nodes give diminishing returns. For the mixed sequence, a performance increase of $3 \pm 1\%$ is noted when increasing the amount of nodes from one to five. The performance increases achieved through spectrogram summation can be explained by the noise-mitigating effects of coherently summing the subjects' micro-Doppler signatures, which will be particularly noticeable when the subject becomes stationary.

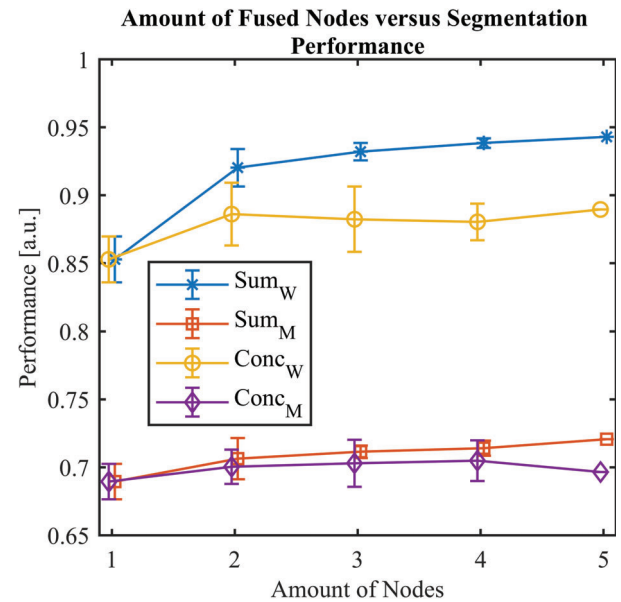


Fig. 2 Segmentation performance of the proposed method vs amount of fused radar nodes for 2 methods of fusion and for 2 sequence types. 'Sum' refers to summation of spectrograms, 'Conc' refers to their vertical concatenation, subscripts 'W' and 'M' refer to sequence types *Walk and Stop*, and '*mix 030*' respectively. Refer to Table 1 for sequence descriptions.

Figures 3 and 4 display a breakdown of performance for both the proposed segmentation method and STA/LTA over different types of sequences in the TUD data set. Parameters are optimised for the *Walk and Stop* sequence and the '*mix 030*' sequence respectively, and applied to all the other sequences. Both methods give comparable results, and it is noted that optimising on the mixed sequence results in a better performance overall, at the cost of a decrease in performance for the simpler *Walk and Stop* sequences.

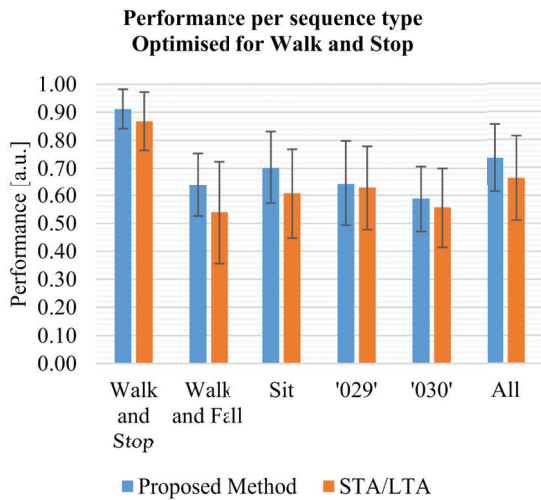


Fig. 3 Segmentation performance for various sequences in the TUD data set and for two segmentation methods. Refer to Table 1 for sequence descriptions. 'All' refers to all sequences.

Lastly, Figure 5 shows the effects of signal-to-noise ratio (SNR) on segmentation performance for both methods. SNR is controlled by adding complex-valued Additive White Gaussian Noise (AWGN) to the signal in the frequency bin corresponding to the centre frequency, obtained after performing the first FFT described in Section 2. The performance for the proposed method decreases less rapidly with decreasing SNR than the method based on STA/LTA. This is possibly attributable to the parameter σ_3 in the STA/LTA method which is intended to serve as a bandwidth threshold for an activity end-point. This parameter is not adaptive and thus, for low SNR, can prevent activity end-points from being detected as noise may cause the bandwidth to remain above the threshold.

6 Conclusion

In this work, segmentation of continuous sequences of human activities is explored through the application and comparison of two methods. The first of these methods is proposed in this work and constitutes the extraction of Rényi entropy from an input spectrogram, and the subsequent evaluation of

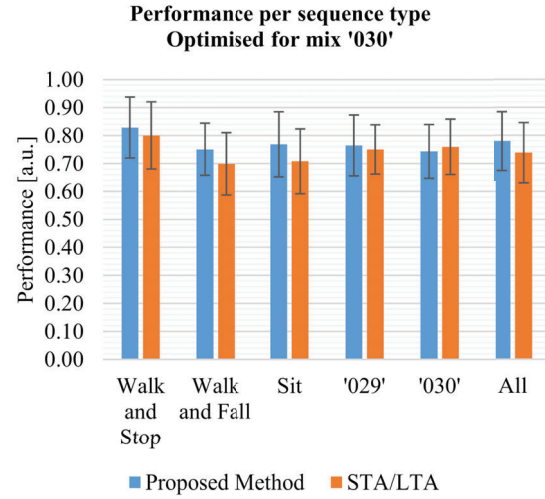


Fig. 4 Segmentation performance for various sequences in the TUD data set and for two segmentation methods. Refer to Table 1 for sequence descriptions. 'All' refers to all sequences.

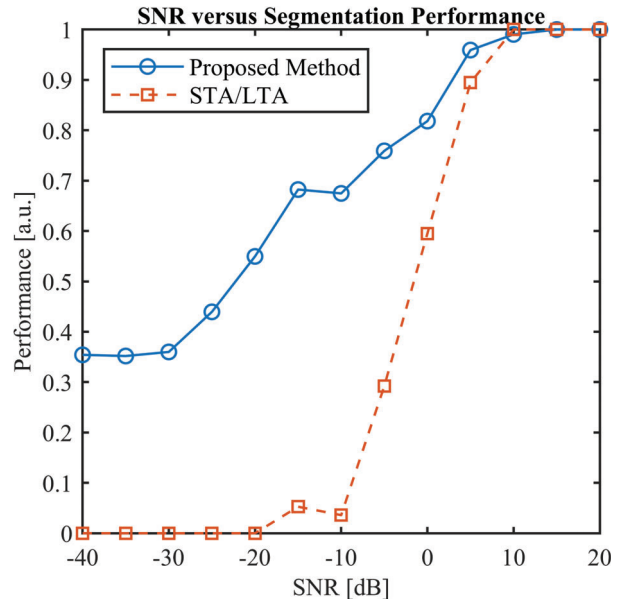


Fig. 5 Segmentation performance versus signal-to-noise ratio (SNR) for a sequence of walking and stopping.

said entropy for transition points. Segmentation accuracy is gauged in different contexts, and improvement of the proposed method over the reference STA/LTA method is noted in the following two cases. Firstly, when applying method parameters optimised on one data set to a different data set, an average

performance improvement of 11 percentage points is achieved, with lower and upper bounds of -11 and $+42$ percentage points respectively. This indicates improved portability of the proposed method parameters. Secondly, when decreasing the SNR of the input spectrograms, the performance of the proposed method declines less rapidly than the reference method, indicating improved noise resilience. Additionally, it is shown that sensor fusion through spectrogram summation results in increased segmentation performance of up to $10 \pm 2\%$ using the proposed method.

In future work, the influence of varying SNR on performance may be investigated further by implementing adaptive features in the proposed method. Since the parameter α influences the relative contribution of high and low values to the entropy, it is expected that it will have a noise-mitigating effect on performance. Furthermore, sensor fusion in this work has been examined by altering the quantity of sensors, but different geometries may give interesting insight in maximising performance whilst minimising sensor utilisation. A valuable addition to the proposed method would be to allow for different levels of 'granularity' in segmentation, i.e. a user-defined threshold as to what constitutes a 'true' transition, as this is a subjective matter in reality.

Finally, the end goal of segmentation is to improve the overall classification accuracy of continuous sequences. An abstract measure of performance is used in this work to enable a preliminary comparison of sequences and methods, but classification accuracy should be a final metric to strive towards.

Acknowledgements

The authors are grateful to the Dutch Research Council (NWO) for support through the project *RAD-ART* (Radar-aware Activity Recognition with Innovative Temporal Networks).

References

- [1] G. Su, N. Petrov, and A. Yarovoy, "Dynamic Estimation of Vital Signs with mm-wave FMCW Radar," in *2020 17th European Radar Conference (EuRAD)*. Utrecht: IEEE, jan 2021, pp. 206–209.
- [2] K.-C. Peng, M.-C. Sung, F.-K. Wang, and T.-S. Horng, "Noncontact Vital Sign Sensing Under Nonperiodic Body Movement Using a Novel Frequency-Locked-Loop Radar," *IEEE Transactions on Microwave Theory and Techniques*, vol. 69, no. 11, pp. 4762–4773, nov 2021.
- [3] Z. Ni and B. Huang, "Open-Set Human Identification Based on Gait Radar Micro-Doppler Signatures," *IEEE Sensors Journal*, vol. 21, no. 6, pp. 8226–8233, mar 2021.
- [4] F. Fioranelli, J. Le Kernec, and S. A. Shah, "Radar for Health Care: Recognizing Human Activities and Monitoring Vital Signs," *IEEE Potentials*, vol. 38, no. 4, pp. 16–23, jul 2019.
- [5] N. Honma, D. Sasakawa, N. Shiraki, K. Murata, T. Nakayama, and S. Iizuka, "A State-Machine-Based Approach for Human Activity Classification Using MIMO Radar," in *2021 International Symposium on Antennas and Propagation, ISAP 2021*, oct 2021, pp. 1–2.
- [6] X. Qiao, G. Li, T. Shan, and R. Tao, "Human Activity Classification Based on Moving Orientation Determining Using Multistatic Micro-Doppler Radar Signals," *IEEE Transactions on Geoscience and Remote Sensing*, pp. 1–15, 2021.
- [7] R. Hernangómez, T. Visentin, L. Servadei, H. Khodabakhshandeh, and S. Stańczak, "Improving Radar Human Activity Classification Using Synthetic Data with Image Transformation," *Sensors*, vol. 22, no. 4, feb 2022.
- [8] R. G. Guendel, F. Fioranelli, and A. Yarovoy, "Distributed radar fusion and recurrent networks for classification of continuous human activities," *IET Radar, Sonar and Navigation (accepted)*, p. 12, 2 2022.
- [9] M. G. Amin and R. G. Guendel, "Radar classifications of consecutive and contiguous human gross-motor activities," *IET Radar, Sonar & Navigation*, vol. 14, no. 9, pp. 1417–1429, sep 2020.
- [10] S. Z. Gurbuz and M. G. Amin, "Radar-based human-motion recognition with deep learning: Promising applications for indoor monitoring," *IEEE Signal Processing Magazine*, vol. 36, no. 4, pp. 16–28, 2019.
- [11] A. Gorji, H.-U.-R. Khalid, A. Bourdoux, and H. Sahli, "On the Generalization and Reliability of Single Radar-Based Human Activity Recognition," *IEEE Access*, vol. 9, pp. 85 334–85 349, 2021.
- [12] Z. Yang, H. Wang, P. Ni, P. Wang, Q. Cao, and L. Fang, "Real-time Human Activity Classification From Radar With CNN-LSTM Network," in *2021 IEEE 16th Conference on Industrial Electronics and Applications (ICIEA)*, Chengdu, China, aug 2021, pp. 50–55.
- [13] E. Kurtoglu, A. C. Gurbuz, E. A. Malaia, D. Griffin, C. Crawford, and S. Z. Gurbuz, "ASL trigger recognition in mixed activity/signing sequences for rf sensor-based user interfaces," *IEEE Transactions on Human-Machine Systems*, pp. 1–14, 2021. [Online]. Available: <https://github.com/ci4r/ASL-Sequential-Dataset>
- [14] H. Li, A. Shrestha, H. Heidari, J. Le Kernec, and F. Fioranelli, "Bi-LSTM Network for Multimodal Continuous Human Activity Recognition and Fall Detection," *IEEE Sensors Journal*, vol. 20, no. 3, pp. 1191–1201, 2020.
- [15] R. G. Guendel, M. Unterhorst, F. Fioranelli, and A. Yarovoy, "Dataset of continuous human activities performed in arbitrary directions collected with a distributed radar network of five nodes," Nov 2021. [Online]. Available: https://data.4tu.nl/articles/dataset/Dataset_of_continuous_human_activities_performed_in_arbitrary_directions_collected_with_a_distributed_radar_network_of_five_nodes/16691500/2
- [16] A. Rényi, "On measures of information and entropy," *Proceedings of the fourth Berkeley Symposium on Mathematics, Statistics and Probability*, p. 547–561, 1960.
- [17] M. Liuni, A. Röbel, M. Romito, and X. Rodet, "Rényi information measures for spectral change detection," in *ICASSP, IEEE International Conference on Acoustics, Speech and Signal Processing - Proceedings*, 2011, pp. 3824–3827.